Conference paper

Matthew R. Golder*, Lev N. Zakharov and Ramesh Jasti

Stereochemical implications toward the total synthesis of aromatic belts

Abstract: The synthesis of carbon nanotube (CNT) fragments has long captivated organic chemists, despite the simplistic, symmetric nature of the requisite achiral targets. Such molecules hold the potential to allow for the synthesis of homogeneous CNTs, rendering their properties more suitable for advanced applications in electronics and sensing. The [n]cycloparaphenylene family, comprised of molecules with para-linked phenyl rings in a contiguous macrocycles, represents a major landmark towards achieving absolute control of CNT architecture from the bottom-up. Attempts towards accessing the [n]cyclacene and [n]cyclophenacene families, both of which are comprised of double-stranded macrocyclic belts, have only recently been successful, however. These targets have been plagued by unstable, strained intermediates and stereochemical pitfalls that have largely thwarted accessing these fascinating structures. Herein, we disclose our synthetic strategy toward overcoming several stereochemical challenges en route to [n]cyclophenacenes via highly substituted [n]cycloparaphenylene precursors.

Keywords: carbon nanotubes; chirality; cyclophanes; diastereoselectivity; IUPAC-SOLVAY International Award for Young Chemists; macrocycles; polycyclic aromatics.

Introduction

Long before the discovery of carbon nanotubes in the early 1990s, significant efforts were made to synthesize rigid, double-stranded CNT fragments that are commonly referred to as "aromatic belts" [1–4]. Like members of the [n]cycloparaphenylene family, the envisaged [n]cyclacene and [n]cyclophenacene targets (Fig. 1, marked in red) are the smallest rigid unit cycles of zigzag and armchair CNTs, respectively (Fig. 1, left). These molecules are deceivingly complex in nature; despite their lack of stereochemical centers, intermediates leading to the proposed highly symmetric, achiral targets are often rich in stereochemistry. These cyclic molecules are also prized for their severely distorted and strained aromatic systems with inward facing pi-orbitals (Fig. 1, right). Elegant work from the Nakamura group has allowed access to a fullerene-derived [10] cyclophenacene through systematic, top-down degradation of C_{60} fullerene (Scheme 1) [5]. While the phenacene in this example is electronically equivalent to a cyclophenancene, structurally it differs due to the lack of an open cavity.

*Corresponding author: Matthew R. Golder, Department of Chemistry and Biochemistry and Material Science Institute, University of Oregon, Eugene, OR 97403, USA; and Department of Chemistry, Massachusetts Institute of Technology, Cambridge, MA 02139, USA, e-mail: goldermr@mit.edu
Lev N. Zakharov: CAMCOR – Center for Advanced Materials Characterization in Oregon, University of Oregon, Eugene, OR 97403, USA
Ramesh Jasti: Department of Chemistry and Biochemistry and Material Science Institute, University of Oregon, Eugene, OR 97403, USA
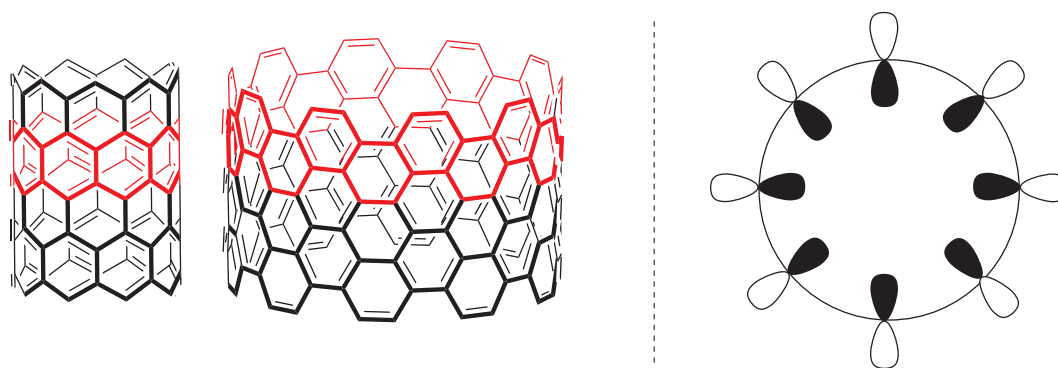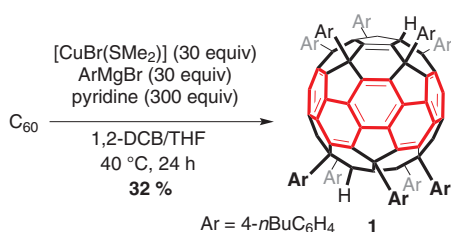
Fig. 1: Zigzag and armchair nanotubes (left), radially oriented p-orbitals (right).


Scheme 1: Nakamura's top-down approach to C_{60} derived [10]cyclophenacene **1**.

Predictions of instability stemming from low singlet-triplet gaps have not dissuaded synthetic chemists from pursuing $[n]_x$cyclacenes, where n defines the ring size(s) and x defines the number of units in the macrocycle, as several accounts on the synthesis of their macrocyclic precursors have been reported [3, 6]. Work from the Stoddart [7–9], Cory [10, 11], and Schlüter [12, 13] laboratories describe the assembly of several oxygenated macrocycles via facial-selective Diels-Alder cycloaddition reactions en route to various cyclacene targets. Upon assembly of kohnkene **4** [7] from **2** to **3**, Stoddart was able to affect partial deoxygenation [8] with $TiCl_4$ and $LiAlH_4$ to deliver **5**. Further dehydration with acetic anhydride and HCl led to **6** (after in situ isomerization), which could not be further oxidized to $[6]_{12}$cyclacene **7**, presumably due to the inability to build in the remainder of the required strain or the instability of the product under the reaction conditions (Scheme 2).
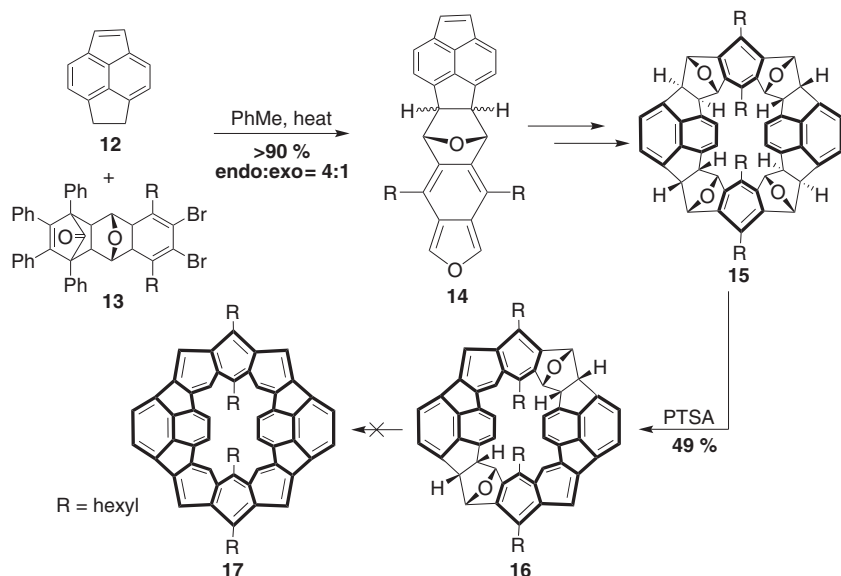
The Cory group was also plagued by the same type of issues with late stage oxidations encountered by the Stoddart lab (Scheme 3). Upon assembling **10** in 69 % from **8** to **9** [10], treatment with a variety of
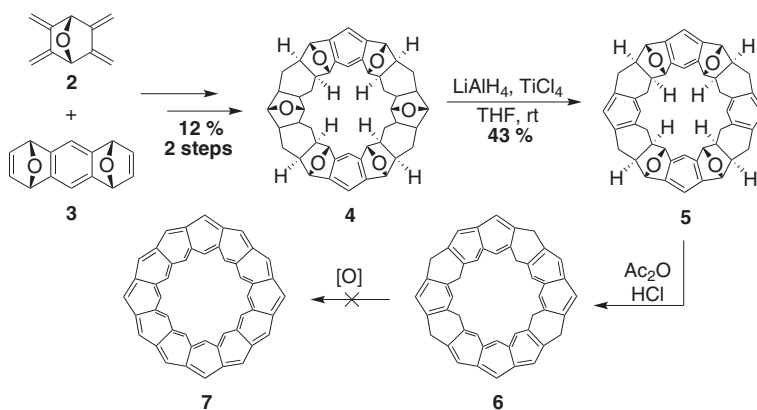
Scheme 2: Stoddart's attempt towards $[6]_{12}$cyclacene **7**.
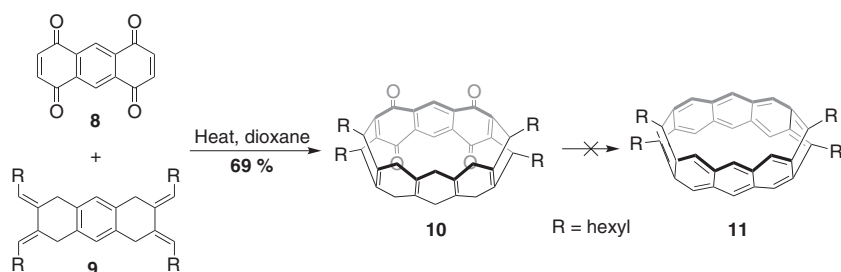
**Scheme 3:** Cory's attempt towards [6]$_8$cyclacene.

Scheme 4: Schlüter's attempt towards buckybelt **17**.

oxidants, such as DDQ, *m*CPBA/*p*TsOH, or PCC only lead to partially dehydrogenated products rather than [6]$_8$cyclacene **11** [11]. No other reports on further manipulations of this scaffold have been reported.

In Schlüter's system, endo-favored Diels-Alder assembly of **14** proceeded in high yield from **12** to **13**. Following several transformations and separation of the resulting diastereomers, macrocyclization afforded **15** in 25–45 % yield. *p*TsOH was effective in dehydrating **15–16** [12], but further oxidation could not be affected with a variety of Brønstead and Lewis acids [13, 14] (Scheme 4). The Schlüter laboratory reports observing the target C$_{84}$ fragment **17** via mass spectrometry after pyrolysis of an aceylated derivative of **16** [15], but no solution-state characterization of **17** has been reported to date [14]. The observed molecular ion could also simply arise from a rearranged isomer due to the harsh experimental conditions [15].

Until a recent remarkable synthesis by the Itami laboratory utilizing a Wittig macrocyclization followed by a series of Ni-mediated reductive coupling reactions [16], attempts towards the bottom-up syntheses of [*n*] cyclophenacenes had also been unsuccessful. One strategy employed by the Iyoda and Vollhardt laboratories stems from attempted oxidative couplings to stitch together the fjord regions of benzoannulenes (Scheme 5). Initially, Iyoda and Vollhardt were able to independently access the all cis-isomer of **20** via a a nickel-catalyzed trimerization of **18** [17] or cobalt-mediated [2+2+2] cyclotrimerization between **19** and bis(trimethylsilyl) acetylene [18], respectively. Both laboratories also reported the thermal isomerization to benzoannulene **21** [17, 19]. Despite the macrocyclic rigidity of **21**, dehydrogenative cyclizations to form the desired [*n*]cyclophenacenes have been unsuccessful to date. Additionally, Herges and co-workers reported on the failure of
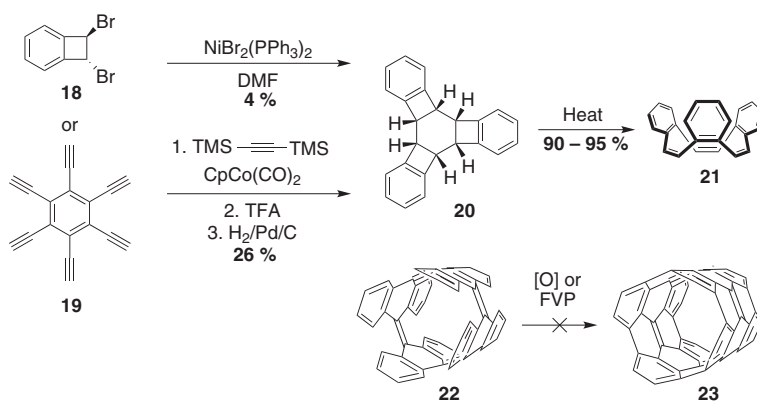
Scheme 5: Attempts from Vollhardt, Iyoda, and Herges towards rigid armchair CNT fragments **21** and **23**.

both flash vacuum pyrolysis (FVP) and oxidative conditions [20] to close the walls of his group's advanced "picotube" **22** to nanotube **23** [21, 22] (Scheme 5).

Due to overwhelming precedence for late-stage, strain-building oxidations to be detrimental in the synthesis of [*n*]cyclacenes and [*n*]cyclophenacenes, we opted to apply our own strain-building methodology as previously realized in the synthesis of [*n*]cycloparaphenylenes ([*n*]CPPs) [23, 24]. For example, in the synthesis of [7]CPP, 16 kcal/mol of strain energy was built up during the macrocyclization step, followed by a late-state *reductive* aromatization event that added an additional 67 kcal/mol of strain energy (Scheme 4). The Müllen group [25–27], as well as our own laboratory [28], have explored the Scholl reaction extensively on substituted [*n*]CPPs. While Müllen and co-workers have shown evidence for oxidative C–C bond formation on extremely large [*n*]CPP backbones (*n* = 21) (**24**), these systems are almost completely unstrained (**25**) and contain substitution patterns to prevent strain-relieving cationic 1,2-phenyl shifts (**26**, Scheme 6) [27]. Hence, we sought a system to explore milder methodology in the context of functionalized [*n*]CPP macrocyclic precursors.

We hypothesized that we could access the [*n*]cyclophenacenes through macrocyclization of olefin functionalized building blocks, followed by a combination of ring-closing metathesis and reductive aromatization
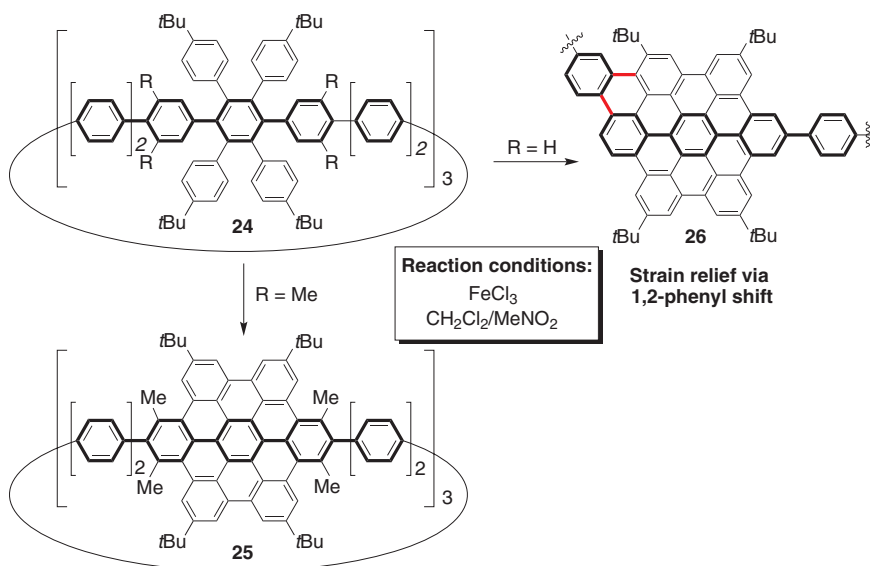
Scheme 6: The variable reactivity of Müllen's large arylated CPPs under Scholl conditions; products depend on the substitution pattern (**25** versus **26**).
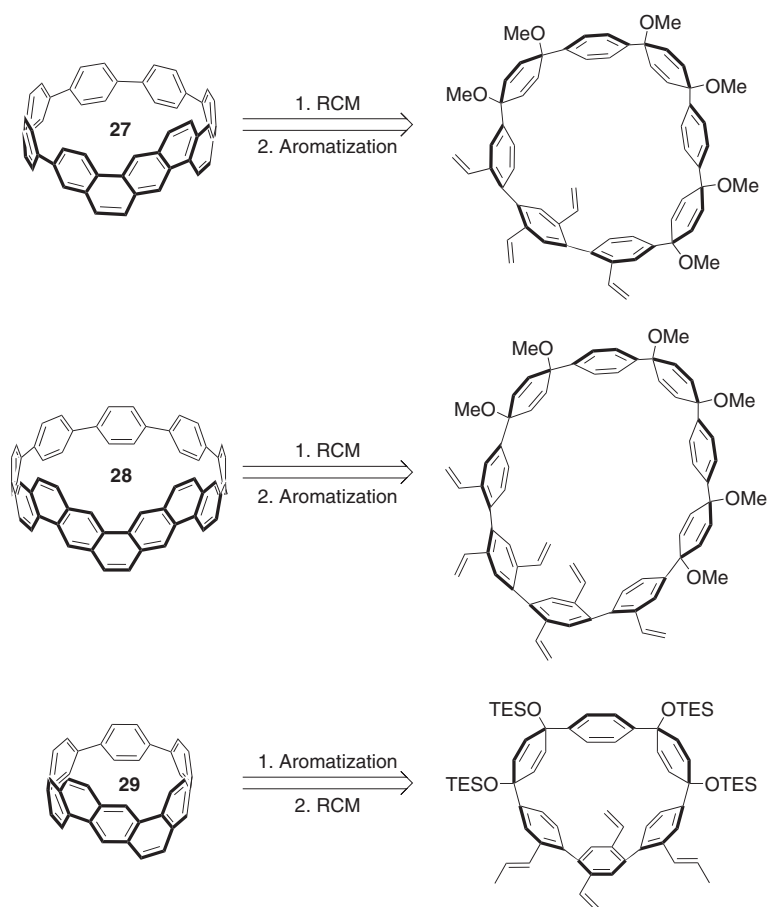
Scheme 7: Retrosynthetic strategy towards aromatic belt fragments **27–29** using ring-closing metathesis.

events. Importantly, unlike in the synthetic attempts from Vollhardt and Iyoda (Scheme 5) we would be separating the ring-forming step (RCM) from the strain-building step (reductive aromatization). In addition, RCM is a redox-neutral process and should not cause cationic, strain-relieving rearrangements. Ring-closing metathesis has been shown to be effective in the synthesis of simple polycyclic aromatic hydrocarbons [29], as well as complex ones such as sumanene [30] and septulene [31]. Indeed, we recently reported on the synthesis of three [*n*]cyclophenacene fragments (**27–29**) through iterative reductive aromatization and RCM processes (Scheme 7), providing proof of principle that aromatic belts can be derived by our new strategy [32].

Retrosynthetic analysis

With a robust strategy to access [*n*]cyclophenacene fragments in hand, we began to consider how to assemble a more elaborate structure such as **30** (Scheme 8). Similar to precursors for nanohoops **27–29**, the presence of syn relative stereochemistry across all cyclohexadiene moieties plays an important role in forming the requisite molecules before any macrocyclization steps. One must also be conscious of the quaternary carbon stereochemistry in the corresponding macrocyclic precursor (Scheme 8). In the case of **31**, all of the stereo-centers are (*S*) and "matched", predisposing all the olefins to undergo productive ring-closing metathesis. In a "mismatched" case, however, where cyclohexadiene rings with opposite stereochemical configurations (i.e. **32**) are in a macrocycle, not all of the necessary ring formations can occur. In such a case, partially closed products such as **33** will form, preventing belt formation upon reductive aromatization. Thus, only cyclohexadiene rings with the same stereochemical configuration, either (*S,S*) or (*R,R*) ought to be assembled
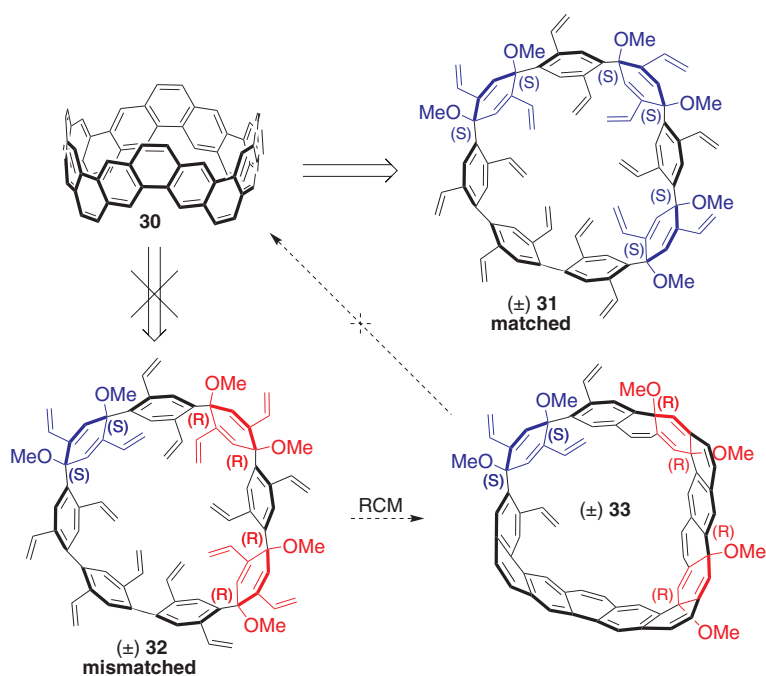
Scheme 8: Retrosynthetic analysis of [*n*]cyclophenacene **30**. To access **30**, cyclohexadiene rings in the macrocyclic precursor must be of the same stereochemical configuration (**31**) to ensure all of the olefins can undergo productive RCM reactions.

together, to avoid scenarios such as **33** where complete ring closure is not possible. In order to construct an appropriate macrocycle, one needs to synthesize the necessary chiral building blocks in an optically pure fashion. Importantly, the presence of any number of "mismatched" macrocycles (such as **32**) could present downstream issues with purification.

Diastereoselective nucleophilic additions to *p*-Quinols

Despite advances allowing for the stereoselective addition of nucleophiles to acyclic carbonyls [33–35] less is known about the origin of selectivity for additions to cyclic conjugated ketones [36]. Of particular interest to the Jasti laboratory are diastereoselective additions of aryl nucleophiles to 4,4-disubstituted 2,5-cyclohexadienones to form 1,4-dihydroxycyclohexa-2,5-diene systems, which are the formal addition products of a two-fold nucleophilic addition to *p*-benzoquinone (Scheme 9). Related studies by Liotta and co-workers [37, 38] provided precedence for controlling the facial selectivity of 1,4-addition to in situ generated quinol alkoxides (Scheme 9). Addition of methylmagnesium chloride to **34** afforded **35**, where the Grignard reagent was directed to the same face as the alkoxide [37]. Substituting a more basic (and coordinatively saturated) organocuprate for the Grignard reagent left one face of the quinol electrostatically
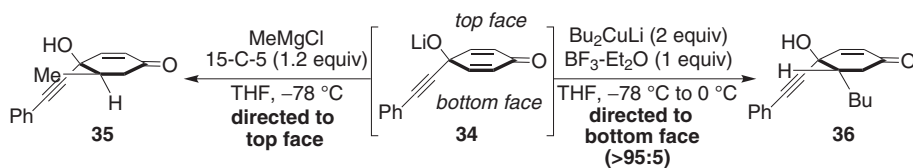
Scheme 9: Diasereoselective 1,4-additions to *p*-quinol **34** controlled by electrostatics.
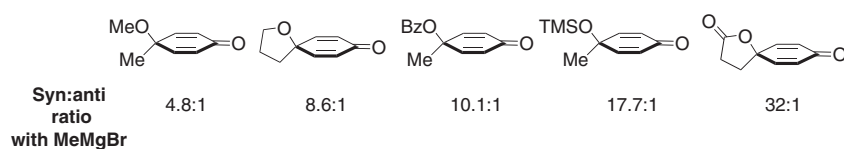
Fig. 2: Facial selectivity for the syn diastereomer increases with larger dipole moments.
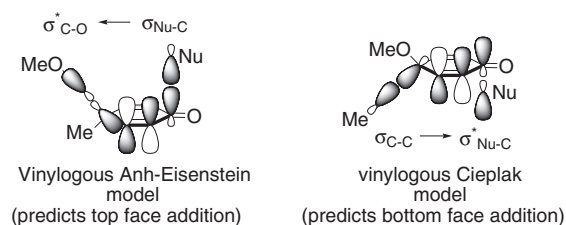

Fig. 3: Neither model accurately predicts the stereoselectivity of 1,2-additions to 4,4-disubstituted 2,5-cyclohexadienones.

shielded, forcing the incoming nucleophile to add in a 1,4 fashion from the opposite face, affording the opposite diastereomer **36** [38].

Wipf and co-workers then used the latter findings from the Liotta group to control facial selectivity of 1,2-additions to 4,4-disubstituted 2,5-cyclohexadienones [36, 39]. They initially observed a stark difference in facial selectivity for a variety of 4-alkoxy and 4-acyloxy substituted *p*-quinols (Fig. 2). In almost all of the cases studied, anti addition that positioned the nucleophile on the face opposite the polar substituent dominated.

Two models were initially considered, but neither one accounted for both the facial selectivity and the dramatic differences in diastereomeric ratios between the different substrates. A modified Anh-Eisenstein model would actually predict preference for addition to the same face as the polar 4-alkoxy or 4-aceyloxy substituent due to favorable overlap between the forming σ_{Nu-C} bond and the σ^*_{C-O} of the polar group. While this model can discern between 4-alkoxy and 4-aceyloxy substituents, again it fails to predict the correct facial selectivity (Fig. 3). A modified Cieplak effect where donation of the 4-alkyl or 4-aryl σ_{C-C} stabilizes the antiperiplanar σ^* of the forming Nu−C bond. Despite explaining the correct facial selectivity, changing the polar substituent should not dramatically affect the donation ability of σ_{C-C} (Fig. 3). Thus, this model too fails to completely explain the observed experimental results [36].

The Wipf group then turned to an inherent difference between their 4,4-disubstituted 2,5-cyclohexadien-ones: dipole moment. As in Liotta's previous examples, electrostatics alone can dramatically bias the facial selectivity of dienone addition reactions. The dipole moments for a subset of the dienones studied were determined computationally, and a linear relationship was found between the logarithim of the diastereomeric ratio and the computed dipole (μ) [39]. With this "dipole effect" (Fig. 4) model in hand, increasing amounts of the desired syn addition product (with respect to the 4-alkyl substituent) could be obtained by increasing the dipole moment of the polar group.
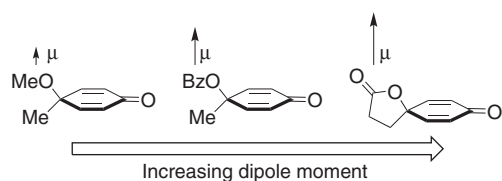

Fig. 4: 4,4-disubstituted 2,5-cyclohexadienones with larger dipole moments (μ, ca. 1.1–3.6 D) led to increasing amounts of the syn 1,2-addition product.

## Development of an electrostatic model for 1,4-addition to dienones

Following work from the Liotta and Wipf laboratories, we speculated that it might be possible to combine the two previously discussed methods to impart facial selectivity for 1,4 dieneone additions of aryl lithium reagents by slowing down the rate of addition to one face of the ketone. While 1,4-syn-dimethoxycyclohexa-2,5-diene systems can be synthesized in two steps from *p*-benzoquinone, the yields and diastereoselectivity are both poor [40]. In addition, this method does not allow access to unsymmetrical systems where the two aromatic rings bear different substituents. We envisioned a stepwise addition procedure that would address all three of these issues. Bromoquinol **37** was used as the primary substrates for our initial studies (Scheme 10). We hypothesized that we would obtain excellent diastereocontrol by first deprotonating *p*-quinol **37** with a base to afford a metal alkoxide. Cooling a solution of **37** to –78 °C, followed by addition of NaH then one equivalent of (4-bromophenyl)lithium gave a 1:1 mixture of **37** and diol **38** [40], even after prolonged reaction time (Scheme II.2). Warming the reaction slowly to room temperature did not afford additional product and just led to an intractable mixture of decomposed material [41]. Clearly, only a portion of the (4-bromophenyl)lithium reagent was reacting with **37**, causing the reaction to stall at ~50 % conversion.

Gratifyingly, when we simply used excess (4-bromophenyl)lithium (2.4 equiv), we observed complete consumption of starting material, as well as a good diastereomeric ratio (syn:anti = 10:1). Our facial selectivity improved (syn:anti = 19:1) by employing NaH as a base, presumably due to the presence of an even more ionic bond (NaO > LiO) (Scheme 11). Decreasing the electrostatic effect further by methylating the alcohol of **37** before addition of (4-bromophenyl)lithium caused the diastereometric ratio to drop (syn:anti = 3:1) [42]. These results are indeed consistent with an electrostatic model where the stereoselectivity of the addition reaction is highly dependent on the strength of the negative charge on one face of the dienone (Scheme 11, inset).

With the ability to begin with **37** and add any (4-halophenyl)lithium reagent diastereoselectively, we first applied this methodology towards the total synthesis of [7]CPP **40** (Scheme 12) via key diene intermediate **39** [42]. Since then, this methodology to construct 1,4-syn-dimethoxycyclohexa-2,5-dienes has been exploited by our laboratory to synthesize a myriad of macrocycles, such as [5]- and [6]CPP, as well as [8]–[12]CPP [43–45].
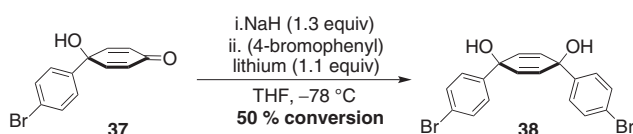
Scheme 10: Attempted diastereoselective synthesis of diol **38**. In the absence of excess aryl lithium reagent, only 50 % conversion is observed to **38**.
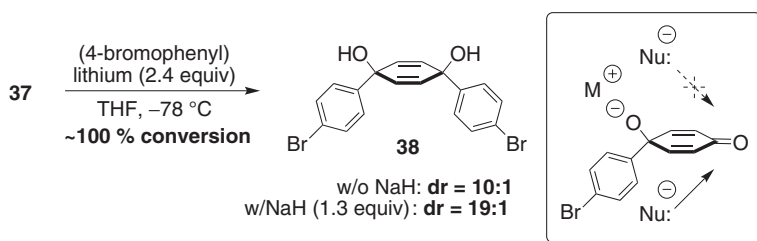
Scheme 11: Diastereoselective synthesis of **38** under electrostatic control. This model (inset) can explain the observed diastereomeric ratios for addition of aryl lithium reagents to **37**.
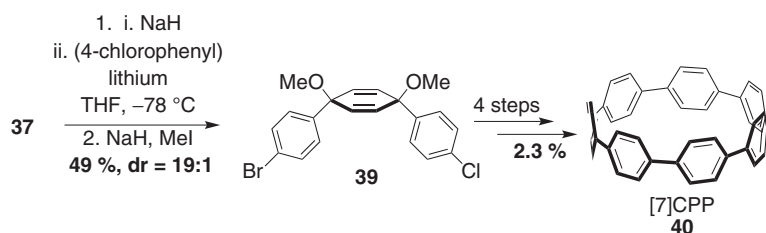
Scheme 12: A general synthetic route to [7]CPP **40** taking advantage of a dipole controlled diastereoselective addition to **37**.

Results and discussion

In order to explore the synthesis of derivatized cycloparaphenylenes for possible application of late-stage ring-closing metathesis chemistry [32], we were intrigued by the possibility of adding functionality to both the cyclohexadiene component and the aryl components of our 1,4-dimethoxycyclohexa-2,5-diene systems (Scheme 8). Ostensibly, we could begin with a prefunctionalized quinone monoketal and a prefunctional-ized 1,4-dibromoarene and employ our well-established methodology to rapidly access highly functional-ized 1,4-syn-dimethoxycyclohexa-2,5-dienes. To access the necessary substituted quinone monoketal **43**, we synthesized **41** via allylation and two-fold Claisen rearrangement of hydroquinone (Scheme 13) [46, 47]. Monomethylation was affected with catalytic sodium nitrite in acidic methanol to afford **42** in 52 % yield [48]. Interestingly, while small amounts of the corresponding quinone (<10 %) were formed during the reaction, presumably due to the competing oxidation of **42** with NO$_2$ [49], the diether was never observed. Oxidative dearomatization of **42** in methanol then delivered ketal **43** 67 % yield.

To synthesize the necessary arene component, two-fold benzylic bromination of 1,4-dibromo-*p*-xylene[29] afforded **44**, which then underwent a two-fold copper-mediated Kumada coupling with vinylmagnesium chloride at the benzylic positions to deliver **45** in 43 % yield. Lithium-halogen exchange of **45** with *n*BuLi (**46**), followed by quenching with either **43** or **43**/MeI afforded **47** and **48**, respectively, after ketal deprotec-tion (Scheme 14).
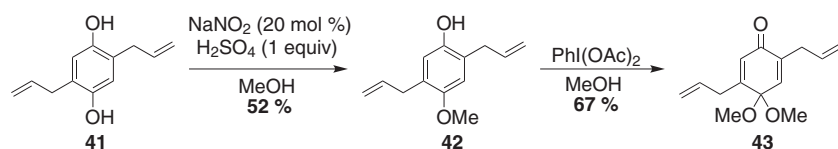
Scheme 13: Synthesis of ketal **43** via monoalkylation and oxidation of **41**.
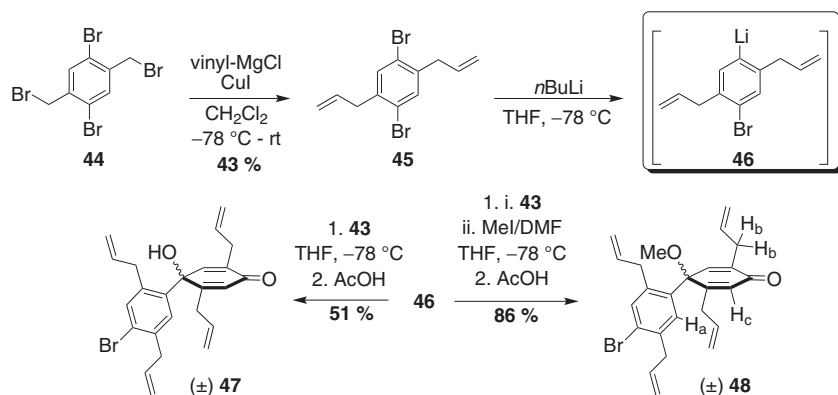

Scheme 14: Synthesis of tetra-allylated ketones **47** and **48** from aryl lithium **46**.

We immediately noticed that both **47** and **48** exhibited extremely broad resonances in their ^{1}H NMR spectrum at room temperature. Many of these resonances sharpened at 70 °C, and we attribute this dynamic behavior to a rare form of atropisomerism between sp^2 and sp^3 hybridized carbons [50–52]. For example, at room temperature we observed broadening of the more downfield aromatic singlet of **48** (Fig. S1), which is presumably the hydrogen closest to the quaternary center (H$_a$, Scheme 14). Surprisingly, however, the broadened allylic sp^3 hydrogens (H$_b$) and broadened sp^2 olefinic hydrogen on the cyclohexadiene ring (H$_c$) are located closest to the carbonyl group, as determined by ^{1}H-^{13}C HMBC NMR experiments on related analog **56** (Fig. S2), as well as ^{1}H-^{1}H COSY NMR experiments of **48** (Fig. S3). In general, all the 4,4-disubstituted 2,5-cyclohexadienones discussed thus far behaved similarly on the NMR timescale; the contents of Figs. S1–S3 serve as representative examples for these class of compounds at both room temperature and 70 °C.

Furthermore, upon the synthesis of **48** (Scheme 15), the formation of minor byproduct **49** was observed as a single diastereomer due to a slight excess of *n*BuLi in the reaction mixture. We believe that this result could have significant stereochemical implications.

It seems possible that the reactive atropisomer *en route* to **48** and **49** is determined by the stereochemical configuration of the cyclohexadiene ring. For example, a pre-determined (*R*) center in the racemic mixture of lithiate during diketone **49** formation (Scheme 16, top) causes the top aromatic allyl group to swing away from the proximal allyl group appended to the cyclohexadiene ring. As a result, attack of electrophile **43** on the pro-(*R*) face minimizes steric clashing between allyl groups. In the case of attack on the pro-(*R*) face (Scheme 16, bottom), sterics prevent formation of the other, "mismatched" diastereomer (vide supra, Scheme 8). This relay of stereochemical information may be responsible for the formation of only a
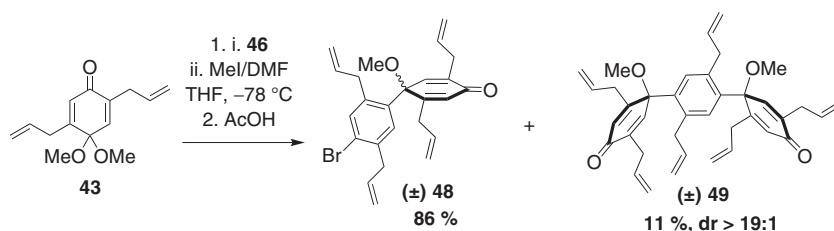
Scheme 15: Synthesis of **49**, an interesting byproduct with significant stereochemical implications.
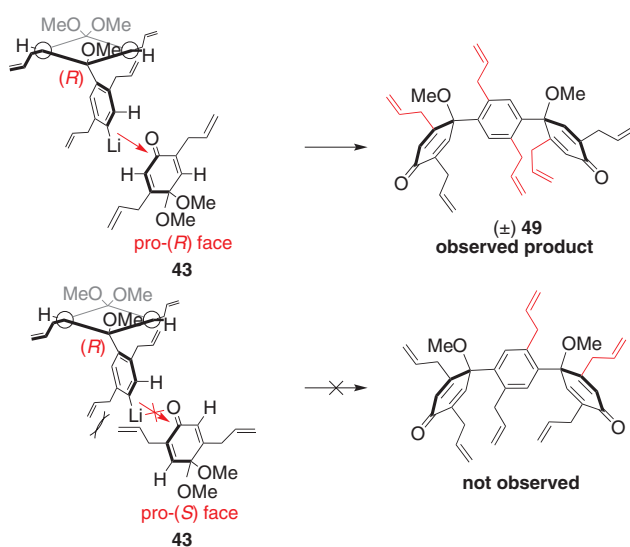
Scheme 16: Stereochemical transfer occurs from the in situ generated organolithium compound to **43** such that all of the necessary olefins of **49** are predisposed to close.
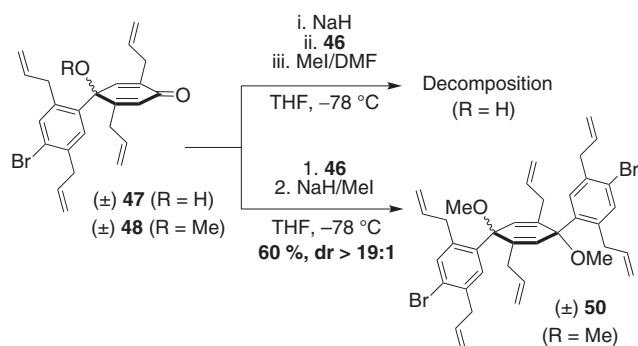
Scheme 17: Two approaches towards the synthesis of **50**. Rates of nucleophilic addition were competitive with decomposition (R = H) unless the dipole moment of the electrophile was attenuated via methylation (R = Me).

single diastereomer, **49,** which is conveniently poised to undergo two C−C bond formations via RCM upon olefin isomerization (Scheme 16). Only the olefins that are poised to form new 6-membered rings via RCM are marked in red in Scheme 16.

Upon isolation of quinol **47**, addition of aryl lithium **46** unfortunately led to rapid decomposition (Scheme 17). On the other hand, methylated quinol **48** allowed for clean addition of **46** (60 % yield, albeit with a reversal of expected diastereoselectivity (anti/syn >19:1) as predicted by our electrostatic model (Scheme 11, inset).

We rationalized the experimental results with both electrostatic and steric arguments. In the case of quinol **47**, addition to the top face (leading to the anti addition product) is slow due to the large dipole from the latent sodium alkoxide. Addition to the bottom face, however, may also be slow due to the sterics imposed by the appended aromatic ring. Regardless of the ring conformation, one of the allyl groups will lie directly underneath the bottom face of the ketone (assuming that the phenyl ring bisects the cyclohexadiene ring). Hence, addition to either face becomes slower than unfavorable pathways, such as decomposition via allylic deprotonation (pK_a ~33 for allylbenzene [53]) by the aryl lithium reagent. On the other hand, methylation of the alcohol (**48**) minimizes the electrostatic effect and increases the rate of addition to the top face, while addition to the bottom face remains slow, resulting in sole addition to afford the anti product. Probing the dominant conformations of **47** and **48** with low temperature NOE experiments were unfortunately unsuccessful and did not provide us with any additional insight to the orientation of the aryl ring with respect to the cyclohexadiene ring. Cooling to −40 °C, however, did lead to sharpening of the ^{1}H NMR resonances for dienones **47** and **48**, suggestive of a major conformation being adopted at lower temperatures (for **48**, Fig. S4). Since the dienones discussed in this section were introduced to the aryl lithium species at room temperature, rather than at −78 °C, multiple conformations could have been present under the actual reaction conditions. In the future, it may be useful to precool the ketones to −78 °C, although there is the obvious possibility that the dominant atropisomer may not improve the status quo.

To study the effect of nucleophile substitution on facial selectivity, (4-bromophenyl)lithium was added to methylated quinol **48** and TMS-protected quinol **51** (Scheme 18). In the former example, unsymmetric 1,4-syn-dimethoxycyclohexa-2,5-diene **52** was isolated in 46 % yield (syn:anti ~4:1), while the latter example afforded **53** (55 % yield brsm; syn:anti ~3:1). In the case of **53**, the tertiary silyl ether was somewhat sensitive to the aryl lithium reagent, leading to recovery of both TMS-quinol **51** and deprotected **47**. For both systems, the diastereomers could not be separated and the diastereomeric ratios were determined by ^{1}H NMR integrations of either the methyl ether or silyl ether regions, respectively. We have tentatively assigned the more upfield, shielded methyl ether and trimethylsilyl resonances to the anti diastereomer, as it is plausible to assume that, at least based on the X-ray crystallographic data for similar adduct **50** (Fig. S6), these groups are situated in the shielding cone of the arene directly across the cyclohexadiene ring. Surprisingly, unlike Wipf's systems [39], there was almost no difference in selectivity between the methylated (**48**) and silylated (**51**) ketones.
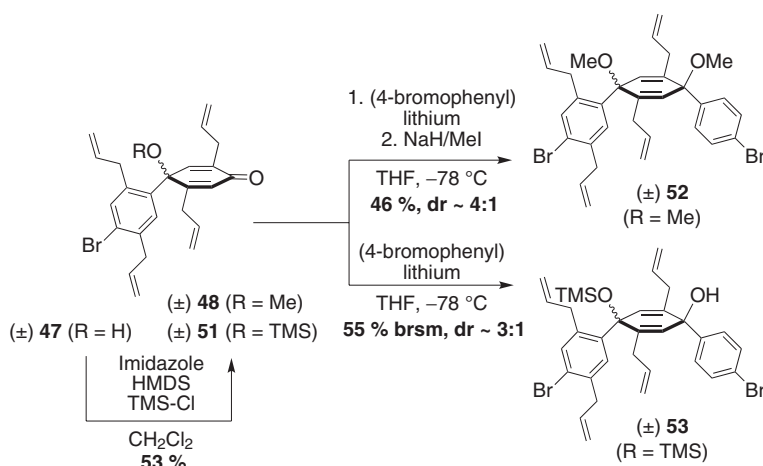
Scheme 18: Use of an unsubstituted nucleophile increased rate of addition to the bottom face, affording syn stereoisomers **52** and **53**.

Thus, while the substitution pattern of the dienone is certainly important, the size of the incoming nucleophile plays a key role as well, since the use of less sterically demanding nucleophile (4-bromophenyl)lithium gave a reversal in selectivity in both cases presented.

To follow up on these observations, we next wanted to examine the effect of arene substitution pattern on both the dienone and the nucleophile components. We first synthesized a methyl ether derived from 1,4-dibromo-2,5-dimethylbenzene (**55**, 76 % yield) (Scheme 19) by nucleophilic addition of (4-bromo-2,5-di-methylphenyl)lithium (**55**+*n*BuLi) to ketal **43**, followed by in situ methylation. Upon acid catalyzed deprotection, a nucleophilic addition of another equivalent of **55**/*n*BuLi to ketone **56** afforded **57** in 62 % yield after in situ methylation. Not surprisingly, we observed a diastereomeric ratio of >19:1 in favor of the anti stereoisomer, which is consistent with what was observed for a similar system with larger allyl substituents on the arene components (**50**, Scheme 17). The stereochemical configuration of the major diastereomer was unequivocally determined by X-ray crystallographic analysis (Fig. S7).

It was hypothesized that use of ortho substitution, rather than para substitution, would increase the rate of addition to the bottom face by alleviating sterics, thus leading to the desired syn diastereomer. Addition of (4-bromo-2,3-dimethylphenyl)lithium, derived from 1,4-dibromo-2,3-dimethylbenzene **58** [54] and *n*BuLi, to ketal **43** delivered methyl ether **59** in 71 % yield after in situ methylation and acid catalyzed deprotection (Scheme 20). In line with our expectations, addition of another equivalent of **58**/*n*BuLi to methyl ether **59** and methylation of the resulting alkoxide gave **60** in 49 % yield with a much lower anti/syn diastereomeric ratio (2:1) as determined by ¹H NMR spectroscopy (Fig. S5). Isolation of both compounds allowed us to obtain crystal structures of the anti (Fig. S8) and syn (Fig. S9) diastereomers. Indeed, ortho substitution allowed for the formation of the desired 1,4-syn-dimethoxycyclohexa-2,5-diene (syn-**60**), albeit as the minor stereoisomer. The NMR spectra for the two diastereomers (Fig. S5) are consistent with our original assertion that the ethereal groups of the anti isomer resonate more upfield (shielded) and those of the syn isomer resonate more downfield (deshielded).
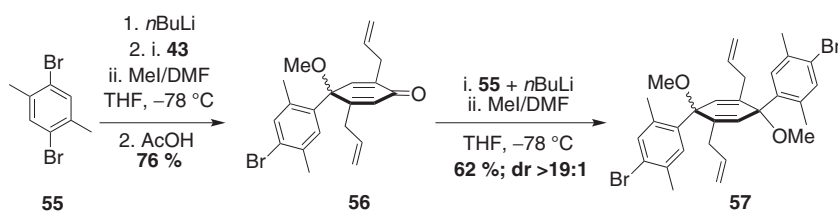
Scheme 19: Smaller *p*-substituents also resulted in exclusive top face addition to deliver anti adduct **57**.
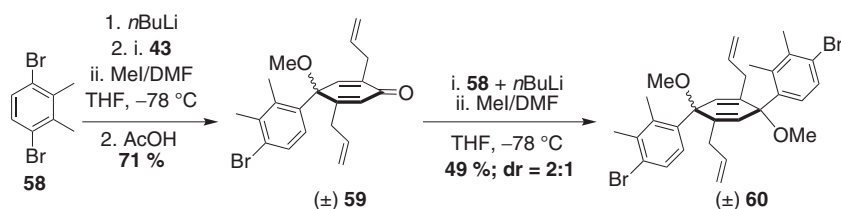
Scheme 20: Use of *o*-substitution increased addition rate to the bottom face and delivered **60** with a diastereomeric ratio of 2:1 (anti/syn).
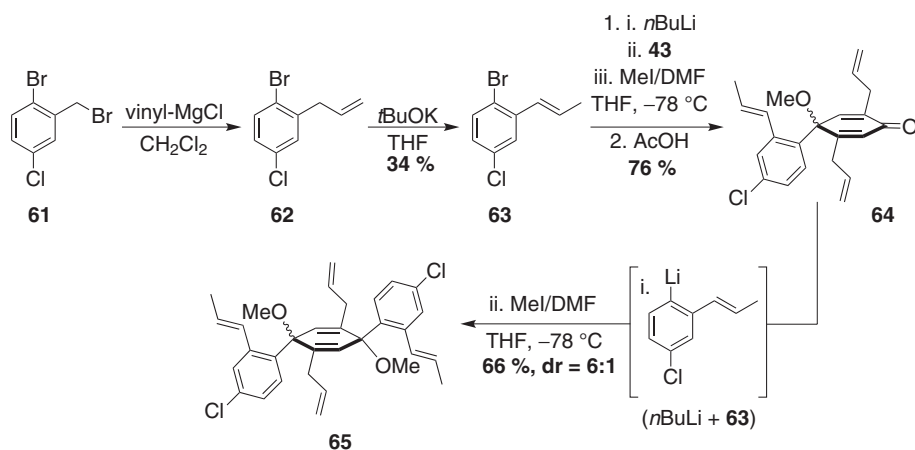
Scheme 21: Propenyl groups on each aryl component led to an erosion of diastereoselectivity in the formation of **65** (anti/syn = 6:1).

Without further optimization, we then examined the diastereoselectivity of an elaborated model that would provide more functionality than a simple methyl group. Inclusion of a single propenyl substituent into both the dienone and the nucleophile components provided additional insight to the stereoselectivity of this class of nucleophilic addition reactions. Beginning with benzylic bromide **61** [55], a copper-catalyzed Kumada cross-coupling with vinylmagnesium chloride (**62**) followed by olefin isomerization afforded **63** (Scheme 21). After lithium-halogen exchange, addition to ketal **43**, and in situ methylation, dienone **64** was easily accessed with functionality on only one side of the arene. In this example, however, the substituent in the lone ortho position is larger than a methyl group. Accordingly, the diastereomeric ratio upon nucleophilic addition to deliver symmetric **65** (66 % yield) was affected by switching to the bulkier propenyl group, increasing the preference for anti addition to 6:1. The stereochemistry of the major diastereomer was determined by X-ray crystallographic analysis (Fig. S10). It seems that while para substitution on the aryl rings leads to high selectivity for the anti isomer, simply increasing the size of the ortho substituent closest to the quaternary center also favors addition to form the anti product (i.e. **59–64**). Although the exact synergy between the different variables that lead to the observed diastereoselectivities is not completely clear at this time, additional experiments to probe the intricacies of the stereochemical outcomes in this class of reactions are currently ongoing.

Conclusion

Herein, we detailed our efforts towards the construction of achiral [*n*]cyclophenacenes proceeding through stereochemically rich building blocks. Based on our previous work involving a ring-closing metathesis end-game strategy, we set out to overcome several stereochemical challenges presented in our proposed total

synthesis. We soon discovered that appropriately substituted intermediates were largely inaccessible with our previous electrostatically-controlled methodology utilized to build other [*n*]CPP derivatives. Based on the scope of substrates explored in an attempt to access highly functionalized 1,4-dimethoxycyclohexa-2,5-dienes, work is underway to hone in on the various factors that dictate the diastereomeric ratio for these types of adducts. It is expected that if functionalized 1,4-dimethoxycyclohexa-2,5-dienes with appropriate stereochemistry can be readily synthesized, ring-closing metathesis can be implemented as a late-stage, ring-forming process to access aromatic belt structures.

References

[1] L. T. Scott. *Angew. Chem. Int. Ed.* **42**, 4133 (2003).
[2] K. Tahara, Y. Tobe. *Chem. Rev.* **106**, 5274 (2006).
[3] D. Eisenberg, R. Shenhar, M. Rabinovitz. *Chem. Soc. Rev.* **39**, 2879 (2010).
[4] P. J. Evans, R. Jasti. *Top. Curr. Chem.* **349**, 1 (2013).
[5] E. Nakamura, K. Tahara, Y. Matsuo, M. Sawamura. *J. Am. Chem. Soc.* **125**, 2834 (2003).
[6] H. S. Choi, K. S. Kim. *Angew. Chem. Int. Ed.* **38**, 2256 (1999).
[7] F. H. Kohnke, A. M. Z. Slawin, J. F. Stoddart, D. J. Williams. *Angew. Chem. Int. Ed.* **26**, 892 (1987).
[8] P. R. Ashton, N. S. Isaacs, F. H. Kohnke, A. M. Z. Slawin, C. M. Spencer, J. F. Stoddart, D. J. Williams. *Angew. Chem. Int. Ed.* **27**, 966 (1988).
[9] U. Girreser, D. Giuffrida, F. H. Kohnke, J. P. Mathias, D. Philp, J. F. Stoddart. *Pure Appl. Chem.* **65**, 119 (1993).
[10] R. M. Cory, C. L. McPhail, A. J. Dikmans, J. J. Vittal. *Tetrahedron Lett.* **37**, 1983 (1996).
[11] R. M. Cory, C. L. McPhail. *Tetrahedron Lett.* **37**, 1987 (1996).
[12] N. Wolf Dietrich, L. Dieter, A. Maribel, A. D. Schlüter. *Chem. Eur. J.* **9**, 2745 (2003).
[13] M. Stuparu, V. Gramlich, A. Stanger, A. D. Schlüter. *J. Org. Chem.* **72**, 424 (2007).
[14] M. Stuparu, L. Dieter, R. Heinz, A. D. Schlüter. *Eur. J. Org. Chem.* **2007**, 88 (2007).
[15] D. Chagit, E. Alexander, A. Walter, S. Amnon, M. Stuparu, A. D. Schlüter. *Chem. Eur. J.* **14**, 1628 (2008).
[16] G. Povie, Y. Segawa, T. Nishihara, Y. Miyauchi, K. Itami. *Science* **356**, 172 (2017).
[17] M. Iyoda, Y. Kuwatani, T. Yamauchi, M. Oda. *J. Chem. Soc., Chem. Commun.* 65 (1988).
[18] R. Diercks, K. P. C. Vollhardt. *J. Am. Chem. Soc.* **108**, 3150 (1986).
[19] L. M. Debra, K. P. C. Vollhardt, W. Stefan. *Angew. Chem. Int. Ed.* **29**, 1151 (1990).
[20] M. Deichmann, C. Näther, R. Herges. *Org. Lett.* **5**, 1269 (2003).
[21] S. Kammermeier, P. G. Jones, R. Herges. *Angew. Chem. Int. Ed.* **35**, 2669 (1996).
[22] S. Kammermeier, P. G. Jones, R. Herges. *Angew. Chem. Int. Ed.* **36**, 2200 (1997).
[23] E. R. Darzi, R. Jasti. *Chem. Soc. Rev.* **44**, 6401 (2015).
[24] M. R. Golder, R. Jasti. *Acc. Chem. Res.* **48**, 557 (2015).
[25] T. Nishiuchi, X. Feng, V. Enkelmann, M. Wagner, K. Müllen. *Chem. Eur. J.* **18**, 16621 (2012).
[26] F. E. Golling, M. Quernheim, M. Wagner, T. Nishiuchi, K. Müllen. *Angew. Chem. Int. Ed.* **53**, 1525 (2014).
[27] M. Quernheim, F. E. Golling, W. Zhang, M. Wagner, H.-J. Räder, T. Nishiuchi, K. Müllen. *Angew. Chem. Int. Ed.* **54**, 10341 (2015).
[28] T. J. Sisto, L. N. Zakharov, B. M. White, R. Jasti. *Chem. Sci.* **7**, 3681 (2016).
[29] M. C. Bonifacio, C. R. Robertson, J.-Y. Jung, B. T. King. *J. Org. Chem.* **70**, 8522 (2005).
[30] H. Sakurai, T. Daiko, T. Hirao. *Science* **301**, 1878 (2003).
[31] B. Kumar, R. L. Viboh, M. C. Bonifacio, W. B. Thompson, J. C. Buttrick, B. C. Westlake, M.-S. Kim, R. W. Zoellner, S. A. Varganov, P. Mörschel, J. Teteruk, M. U. Schmidt, B. T. King. *Angew. Chem. Int. Ed.* **51**, 12795 (2012).
[32] M. R. Golder, C. E. Colwell, B. M. Wong, L. N. Zakharov, J. Zhen, R. Jasti. *J. Am. Chem. Soc.* **138**, 6577 (2016).
[33] D. J. Cram, F. A. A. Elhafez. *J. Am. Chem. Soc.* **74**, 5828 (1952).
[34] N. T. Anh, O. Eisenstein. *Tetrahedron Lett.* **17**, 155 (1976).

[35] D. A. Evans. *Science* **240**, 420 (1988).
[36] P. Wipf, J.-K. Jung. *Chem. Rev.* **99**, 1469 (1999).
[37] K. A. Swiss, D. C. Liotta, C. A. Maryanoff. *J. Am. Chem. Soc.* **112**, 9393 (1990).
[38] K. A. Swiss, W. Hinkley, C. A. Maryanoff, D. C. Liotta. *Synthesis* **1992**, 127 (1992).
[39] P. Wipf, Y. Kim. *J. Am. Chem. Soc.* **116**, 11678 (1994).
[40] R. Jasti, J. Chattacharjee, J. B. Neaton, C. R. Bertozzi. *J. Am. Chem. Soc.* **130**, 17646 (2008).
[41] Attempts to deprotonate quinol **37** at 0 °C also led to an untraceable mixture of decomposed material.
[42] T. J. Sisto, M. R. Golder, E. S. Hirst, R. Jasti. *J. Am. Chem. Soc.* **133**, 15800 (2011).
[43] E. R. Darzi, T. J. Sisto, R. Jasti. *J. Org. Chem.* **77**, 6624 (2012).
[44] P. J. Evans, E. R. Darzi, R. Jasti. *Nat. Chem.* **6**, 404 (2014).
[45] J. Xia, R. Jasti. *Angew. Chem. Int. Ed.* **51**, 2474 (2012).
[46] S. K. Chattopadhyay, B. K. Pal, S. Maity. *Chem. Lett.* **32**, 1190 (2003).
[47] K. C. Majumdar, B. Chattopadhyay, S. Chakravorty. *Synthesis* **2009**, 674 (2009).
[48] C. Gambarotti, L. Melone, C. Punta, S. U. Shisodia. *Curr. Org. Chem.* **17**, 1108 (2013).
[49] E. Bosch, R. Rathore, J. K. Kochi. *J. Org. Chem.* **59**, 2529 (1994).
[50] H. J. Martin, M. Drescher, H. Kählig, S. Schneider, J. Mulzer. *Angew. Chem. Int. Ed.* **40**, 3186 (2001).
[51] D. Casarini, L. Lunazzi, A. Mazzanti. *J. Org. Chem.* **73**, 2811 (2008).
[52] D. Casarini, L. Lunazzi, A. Mazzanti. *J. Org. Chem.* **73**, 6382 (2008).
[53] K. Bowden, R. S. Cook. *J. Chem. Soc., Perkin Trans. 2*, 1407 (1972).
[54] Y.-H. Lai, A. H.-T. Yap. *J. Chem. Soc., Perkin Trans. 2*, 1373 (1993).
[55] D. R. Spring, S. Krishnan, H. E. Blackwell, S. L. Schreiber. *J. Am. Chem. Soc.* **124**, 1354 (2002).